

ORIGINAL ARTICLE

Cell fusion promotes chemoresistance in metastatic colon carcinoma

V Carloni¹, A Mazzocca², T Mello³, A Galli³ and S Capaccioli⁴

Chemoresistance is an important concern in the treatment of metastatic colon cancer. It may emerge through selection of clones that are inherently resistant from the outset or through mechanisms acquired during treatment. Cell fusion represents an efficient means of rapid phenotypic evolution that make cells with new properties at a rate exceeding that achievable by random mutagenesis. Here, we first identified a number of proteins involved in cell fusion using a shotgun proteomics approach, then we investigated the role of these proteins namely tetraspanin CD81/CD9, ADAM10, GTP-binding protein α 13, radixin, myosin regulatory light chain and RhoA in the regulation of colon cancer cell fusion. We also found a previously unrecognized role of ADAM10, G α 13 and RhoA in promoting cell fusion. Finally, we show that the occurrence of cell fusion in a metastatic model of colon carcinoma causes the appearance of cells resistant to both 5-fluorouracil and oxaliplatin. These findings highlight the importance of cell fusion in cancer progression and raise significant implications for overcoming chemoresistance in metastatic colon cancer.

Oncogene (2013) 32, 2649–2660; doi:10.1038/onc.2012.268; published online 2 July 2012

Keywords: colon cancer therapy; RhoA; GTP-binding protein α 13; tetraspanin CD81/CD9; FOLFOX; ADAM10

INTRODUCTION

Survival times of patients with advanced colon cancer have increased over the last decade, primarily as a result of treatment with combinations of cytotoxic agents. However, the clinical benefits of these therapies are short-lived and restricted to subgroups of patients. Resistance to cytotoxic drugs is the main cause of therapeutic failure, which usually recurs with a multidrug resistance (MDR) phenotype shortly after dramatic response to initial treatments. Some molecular mechanisms of drug resistance are known. Two well-characterized drug efflux pumps, P-glycoprotein and MDR-related protein, have been thought to be crucial for MDR. However, the importance of these mechanisms remains still controversial. For example, ectopic expression of these pumps induces partial resistance in comparison with that achieved by long-term drug selection.^{1,2} Clinical studies have also revealed that expression of these pumps was rarely observed and did not necessarily correlate with the outcome in colon cancer.³ Therefore, these proteins cannot completely account for the appearance of a MDR phenotype of colon cancer and other mechanisms must be involved in this process. 5-Fluorouracil (5-FU), leucovorin and oxaliplatin (Oxa) represent a therapeutic regime (FOLFOX) commonly used in the treatment of patients with advanced colon cancer.^{4–6} Resistance to therapy occurs in nearly all patients with metastatic colon cancer, and patients that acquire resistance have a disease progression with few therapeutic options. As the gain of drug resistance involves the acquisition of a new phenotype, we hypothesized that the generation of fused cells in metastatic colon cancer could represent a phenomenon responsible of MDR. In recent years, accumulating experimental evidence has suggested a possible broad involvement of cell fusion during the initiation, progression

and phenotypic diversification of cancer.^{7–9} Cell fusion is a process in which two cells become one by merging their plasma membranes.^{10–12} The role of cell fusion in metastasis has been recently demonstrated. This represents an efficient means of rapid phenotypic evolution during tumor progression that make cells with new properties at a rate exceeding that achievable by random mutagenesis.¹³

In spite of the diversity of cell types that undergo fusion, the underlying cellular processes, including cell–cell adhesion, alignment and membrane mixing, are similar irrespective of the cell type.¹⁴ In this regard, tetraspanins and ADAMs (A Disintegrin And Metalloprotease domain) proteins have been implicated in cell fusion processes. In particular, tetraspanin CD9 and CD81 have been implicated in muscle cell fusion, mononuclear phagocytes and linked to the virus-induced syncytium formation.^{15–17} ADAMs were initially discovered as proteins involved in fertilization, muscle fusion and organ development.^{18,19} In this study, we provide evidence that proteins ADAM10, GTP-binding protein α 13, radixin, myosin regulatory light chain and RhoA promote cell fusion in colon cancer cells. In addition, we demonstrate that cell fusion results in the acquisition of a resistant phenotype to both 5-FU and Oxa, two pharmacological agents commonly employed in the treatment of advanced colon cancer.

RESULTS

Identification of distinct proteins associated with CD81 by shotgun proteomics

Because of the implication of tetraspanin CD81 in cell fusion and in an attempt to identify and characterize the proteins associated with CD81, we immunoprecipitated CD81 from Triton X-100 cell

¹Department of Internal Medicine, Center for Research, Transfer and High Education, DENOthe, University of Florence, Florence, Italy; ²Department of Emergency and Organ Transplantation, Section of Internal Medicine, Allergology and Clinical Immunology, University of Bari Medical School, Bari, Italy; ³Department of Clinical Pathophysiology, Gastroenterology Unit, University of Florence, Florence, Italy and ⁴Department of Experimental Pathology and Oncology, University of Florence, Florence, Italy. Correspondence: Dr V Carloni, Department of Internal Medicine, Center for Research, Transfer and High Education, DENOthe, University of Florence, Largo Brambilla 3, Florence 50134, Italy. E-mail: v.carloni@dmf.unifi.it

Received 25 November 2011; revised 30 April 2012; accepted 1 May 2012; published online 2 July 2012

lysates of human colon cancer cells, SW480. To eliminate background proteins not effectively associated with CD81, we used an IgG1 antibody as control. Any protein identified in both conditions was not considered as a protein associated with CD81. The immunoprecipitated proteins were digested with trypsin and peptides were subsequently identified by shotgun proteomics.²⁰ The proteomic analysis led to the identification of 51 proteins (Supplementary Information Table S1). We found different classes of molecules associated to CD81, including tetraspanin CD9, molecules mediating adhesion with extracellular matrix (that is, integrins), cell-cell adhesion (that is, EpcAM, CD44), signaling proteins (that is, heterotrimeric G protein subunits) and the disintegrin-like metalloproteinase ADAM10. Of the proteins identified in this screen, CD81, CD9 have been implicated in cell fusion, whereas less is known about the role of ADAM10. First, we verified the cellular colocalization of CD81 and CD9 with ADAM10 in SW480 by immunofluorescence and found that CD81 and CD9

colocalize with ADAM10 in punctuate structures (Figure 1a). Then, we addressed the cellular colocalization of CD9 with ADAM10 in the CD81-negative murine colon cancer cells, CT26. Similarly, these cells showed a robust colocalization of CD9 with ADAM10 in punctuate structures (Figure 1b).

The next step was to assess the physical interaction of CD81 and CD9 with ADAM10 by immunoprecipitation experiments. These revealed that CD81 and CD9 are indeed associated with ADAM10, a protein migrating at 78 kD under nonreducing conditions (Figure 1c). Most ADAMs, including ADAM10, possess the typical HEXGHXXGXXH motif at their catalytic site, which is responsible for the zinc-dependent protease activity. We therefore assessed the presence of proteolytic activity associated with CD81 and CD9 by using gelatin zymography. The detection of a collagenolytic band migrating at ~78 kD confirmed the presence of ADAM10 in the CD81/CD9-immunoprecipitated complexes (Figure 1d).

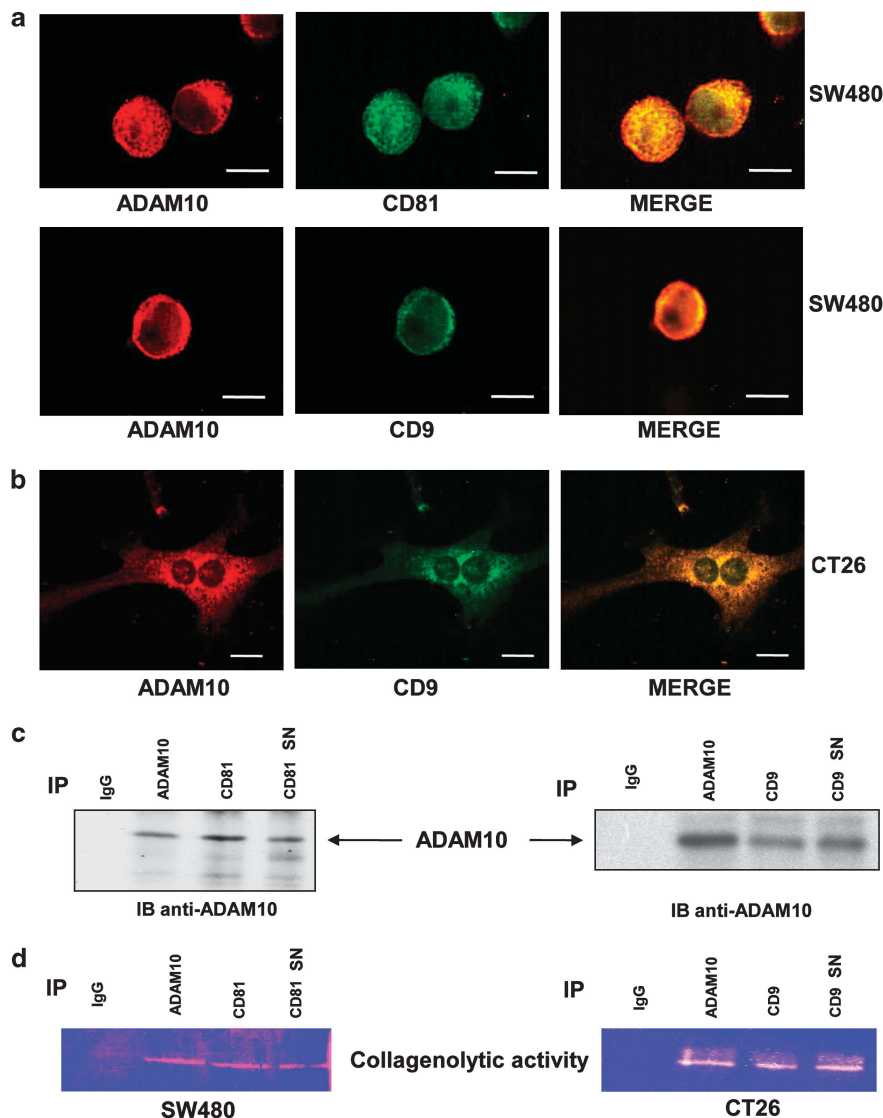


Figure 1. Association of CD81 and CD9 with ADAM10 in colon carcinoma cells. **(a)** Representative images showing colocalization of ADAM10 (red) with CD81 and CD9 (green) in SW480 human colon carcinoma cells. **(b)** Representative images showing colocalization of ADAM10 (red) with CD9 (green) in CT26 murine colon carcinoma cells, scale bars 20 μm. **(c)** Co-immunoprecipitation (IP) of ADAM10 with CD81 in both cell lysates and culture medium supernatants (SN) of SW480 cells (left panel). Co-immunoprecipitation of ADAM10 with CD9 in both cell lysates and culture medium SN of CT26 cells (right panel). **(d)** Immunoprecipitation of CD81 or CD9 followed by gelatin zymography revealed that CD81 and CD9-associated ADAM10 was functionally active in both cell lysates and culture medium SN of SW480 and CT26 cells.

Colon carcinoma cell fusion is promoted by ADAM10 that is stably associated to CD81 and/or CD9

We focused our attention on the role of ADAM10 and its structural domains in regulating cell fusion. Hence, we cloned a bovine ADAM10 cDNA, whose amino-acidic sequence is identical to the human ADAM10, into a plasmid expressing a monomeric red fluorescent protein tagged to ADAM10 (ADAM10-RFP). The ADAM10-RFP cDNA was then ectopically expressed in CT26. We observed the appearance of binucleate or multinucleate CT26 cells when the ADAM10-RFP-transfected CT26 cells were grown in the presence of geneticin, an antibiotic used to select ADAM10-RFP stable transfectants (Supplementary Information Figure S1A). We assumed that this aspect was allegedly due to cell fusion and eventually enhanced by ADAM10 overexpression. Therefore, we next evaluated whether the multinucleated phenotype induced by ADAM10 was restricted only to CT26 cells or whether this was a more general phenomenon. To this end, human colon cancer cells HCT116 not expressing CD81 were stably transfected with ADAM10-RFP and evaluated for the presence of the multinucleated phenotype as performed with ADAM10-RFP-CT26 transfectants. Similar to CT26, HCT116 cells expressing ADAM10-RFP showed the presence of multinucleated cells (Supplementary Information Figure S1B). These findings indicate that ectopic expression of ADAM10 increased the fusogenic competence in both human and murine colon cancer cell types.

To further substantiate the involvement of ADAM10-RFP in promoting cell fusion, we co-cultured CT26-EGFP stable transfectants with CT26-ADAM10-RFP stable transfectants for 2 days. Fused cells were identified by dual color FACScan (BD FACSCalibur, San Jose, CA, USA). As shown in Figure 2a, right panel, ectopic expression of ADAM10-RFP accounted for the presence of a large number of fused cells (28%) in comparison with control (8.9%), left panel, and the subsequent scatter measurement revealed an increase in cell size of fused cells (Figure 2b).

To visualize cell fusion, we take advantage of live-cell imaging. We therefore seeded an equal number of untransfected and ADAM10-RFP-transfected CT26 cells onto a layer of Matrigel and performed time-lapse confocal microscopy for 18 h (64 800 s). The cell mixture was imaged by capturing a single confocal section at the indicated times. A representative animated sequence of the imaged cells is shown in supplementary information Movie S1. As shown in Figure 2c, the cell-cell contact between ADAM10-RFP-CT26 transfectants and untransfected CT26 resulted, in this latter, in altered cell shape (upper and middle panels) and in a disruption of the cell membrane followed by cell fusion (lower panels). Taken together, these results imply that expression of ADAM10 promotes cancer cell fusion.

Reduced expression of CD9 increases cell fusion in the CT26 and HCT116 cells

The role of CD81 and CD9 in cancer cell fusion is at the present barely defined, therefore, we tested whether inhibition of CD9 expression in the CD81-negative CT26 and HCT116 cells would affect their fusion ability. To do so, we used a short hairpin-interfering RNAs (shRNA) targeted against the coding region of the mouse and human *CD9* gene. As shown in Figure 3a, expression of CD9-shRNA results in a reduction of both mRNA and CD9 protein expression levels in CT26 cells as evaluated by flow cytometry and RT-PCR, respectively. A control-shRNA (CTL-shRNA) did not cause a reduction of CD9 expression (Figure 3a). Similarly, expression of CD9-shRNA results in a reduction of both mRNA and CD9 protein expression levels in HCT116 cells (Figure 3b). Notably, the reduced expression of CD9 enhanced the percentage of fused cells in both CT26 and HCT116 cell lines in comparison with CT26 and HCT116 transduced with control-shRNA. Collectively, our data suggest that the presence of CD9 may prevent colon cancer cell fusion.

Cysteine-rich domain of ADAM10 is required for CD81 and CD9 association with ADAM10 and supports colon carcinoma cell adhesion

The findings that ADAM10 promotes cell fusion of CT26 and HCT116 prompted us to investigate whether carcinoma cells attached to the extracellular portion of ADAM10. To study the involvement of ADAM10 domains in promoting cell adhesion, we performed experiments using recombinant ADAM10 truncation mutants and different colon carcinoma cell lines (CT26, SW480 and HCT116). In particular, the recombinant domains of ADAM10 were tagged with EGFP at COOH terminus to allow their detection, and then expressed in COS-7 cells (Figure 4a). To determine the interaction of the recombinant mutants of ADAM10 with tetraspanin CD81, we took advantage by the fact that COS-7 cells were negative for CD81 expression. Hence, we co-expressed EGFP-tagged ADAM10 mutants and the human pcDNA 3.1 vector harboring CD81 in COS-7 cells. The physical association was then analyzed by co-immunoprecipitation in both cell lysates and culture medium supernatants. As shown in Figure 4b, CD81 was detected in immunoprecipitates from cells expressing full-length ADAM10 (ADAM10-EGFP), disintegrin and cysteine-rich domain and cysteine-rich domain alone (Cys-EGFP) but not in those expressing the transmembrane and intracytoplasmic domain (TMCyt-EGFP). Interestingly, we detected the presence of endogenous CD9 in the immunoprecipitates of these variants. This is in agreement with a previous study showing that microvesicles containing both CD81 and CD9 are released by cells in the culture medium.²¹ These results clearly demonstrate the association of CD81 and CD9 with ADAM10. Even more important, our data elucidate a crucial role for the cysteine-rich domain of ADAM10 in mediating association with CD81 and CD9.

A fundamental feature of cell fusion is the juxtaposition of two plasma membranes. To evaluate a possible involvement of ADAM10 in this process, we addressed the ability of CT26 to interact with ADAM10. As shown in Figure 4c, CT26 cells attached to: (1) recombinant disintegrin and cysteine-rich domain, (2) cysteine-rich domain alone and (3) full-length ADAM10. No cell attachment was observed to the transmembrane/cytoplasmic domain. A similar adhesion pattern was observed in analog experiments carried out with SW480 and HCT116 cells.

ADAM10 and CD81 regulate localization of GTP-binding $\alpha 13$

We hypothesize that tetraspanin CD81 and CD9 and ADAM10 contribute to bringing the opposing membranes into close proximity in fusogenic cancer cells and that, in a subsequent step, these proteins can recruit intracellular proteins forming multi-protein complexes at the sites of fusion. To explore this hypothesis, we went back to our proteomic data and focused on GTP-binding protein $\alpha 13$. $G\alpha 13$ acts as a signal transducer for G protein-coupled receptor as well as for non-G protein-coupled receptor. As illustrated in Figure 5a, ADAM10 and CD81 showed a prominent colocalization with $G\alpha 13$ in SW480 cells. A robust colocalization of ADAM10 and CD9 was also observed in CT26 cells (Figure 5b). To learn more about the localization of $G\alpha 13$, we cotransfected a RFP vector with CD81-GFP, as shown in Supplementary Information Figure S2A, and a RFP-tagged $G\alpha 13$ with CD81-GFP (Supplementary Figure S2B). We observed colocalization of RFP- $G\alpha 13$ with CD81-GFP at cellular cortex and induction of cell rounding in CT26 and HCT116 cultured on a two-dimensional glass-bottomed dishes (Supplementary Figure S2B). These data clearly indicate that $G\alpha 13$ takes part in the plasticity of the plasma membrane and the remodeling of the cytoskeleton.

However, a fundamental question remained about how CD81 and ADAM10 are organized in paired living cells plunged in a three-dimensional substrate. To this end, we cotransfected CT26 cells with CD81-GFP and RFP- $G\alpha 13$, suspended them in gelled Matrigel and immediately analyzed by fluorescence microscopy.

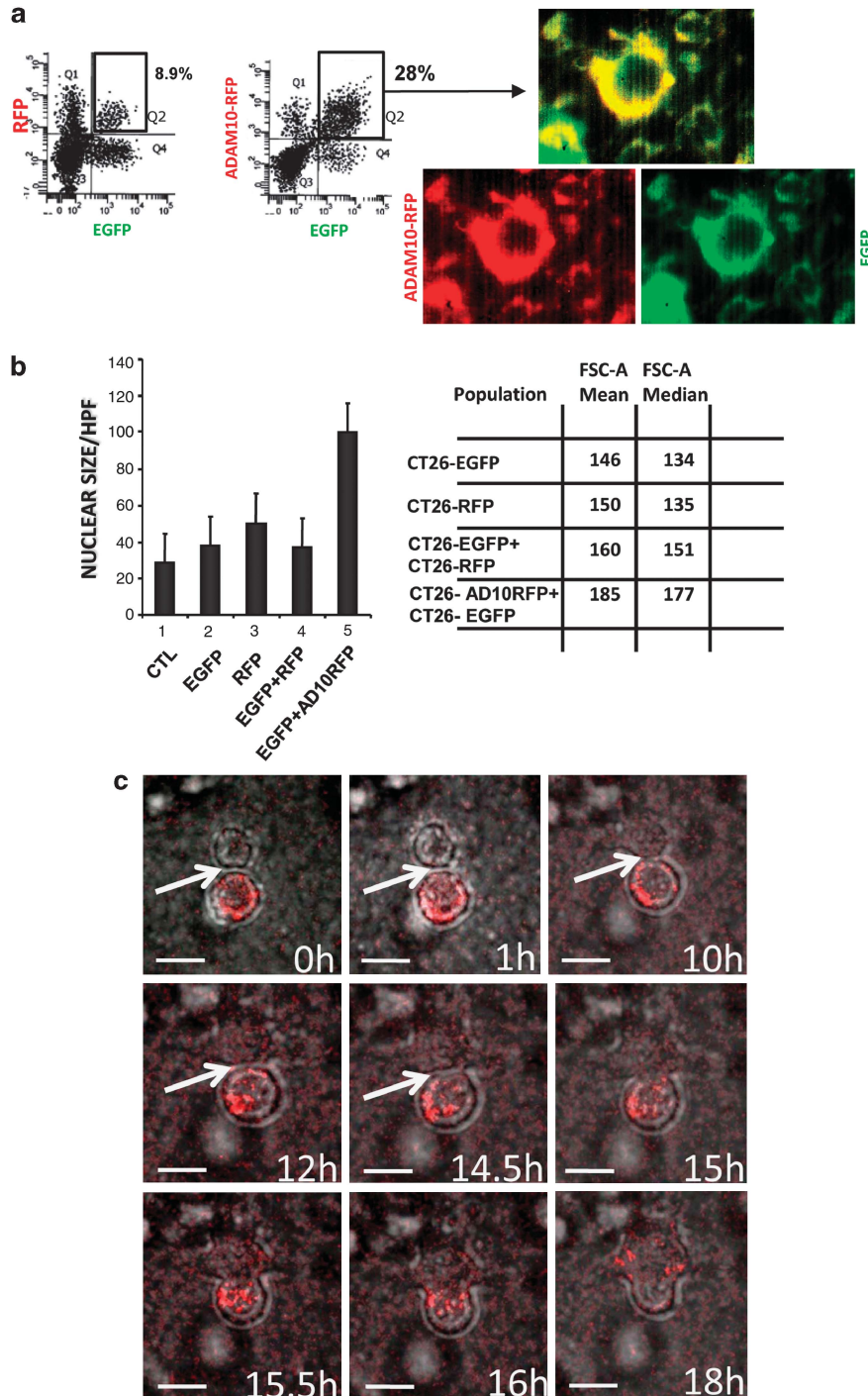


Figure 2. Ectopic expression of ADAM10 promotes cell fusion in colon carcinoma. **(a)** CT26 cells stable transfectants expressing ADAM10-RFP (red image) and CT26 stable transfectants expressing EGFP empty vector (green image) were co-cultured for 2 days and the fused cells (yellow image) were then quantified by dual color FACScan. In the left panel, fluorescence dots in panel Q2 represent cells fused expressing both EGFP and RFP proteins. In the right panel, fluorescence dots in panel Q2 represent cells fused expressing both EGFP and ADAM10-RFP proteins. **(b)** Nuclear size was measured following 4,6-diamidino-2-phenylindole (DAPI), staining of fixed cells (left panel) whereas cell size was measured by flow cytometry as forward scatter (right panel). One representative experiment out of two is shown. **(c)** Tracking of CT26 cell fusion by live-cell imaging. An equal number of non-labeled CT26 and CT26 expressing ADAM10-RFP (red) were mixed, included into a layer of Matrigel and immediately analyzed by time-lapse confocal microscopy for 18 h (see also Supplementary Information, Movie S1). The cell mixture was imaged by capturing a single confocal section at the indicated times (30 min each). Cell-to-cell contact of a CT26 expressing ADAM10-RFP (red) with a non-labeled CT26 is indicated with a white arrow. Cell fusion was observed between a positive ADAM10-RFP-CT26 cell and a non-RFP-labeled CT26 cell. In non-RFP-labeled CT26 cells, the cell-to-cell contact leads to cell shape modifications (upper and middle panels) and consecutively to disruption of the cell membrane (lower panels). In the last panel, immediately after the fusion, ADAM10-RFP was localized in the cytosol of the non-labeled CT26 cell, indicating an exchange of the ADAM10-RFP between cells. Scale bars 20 μ m.

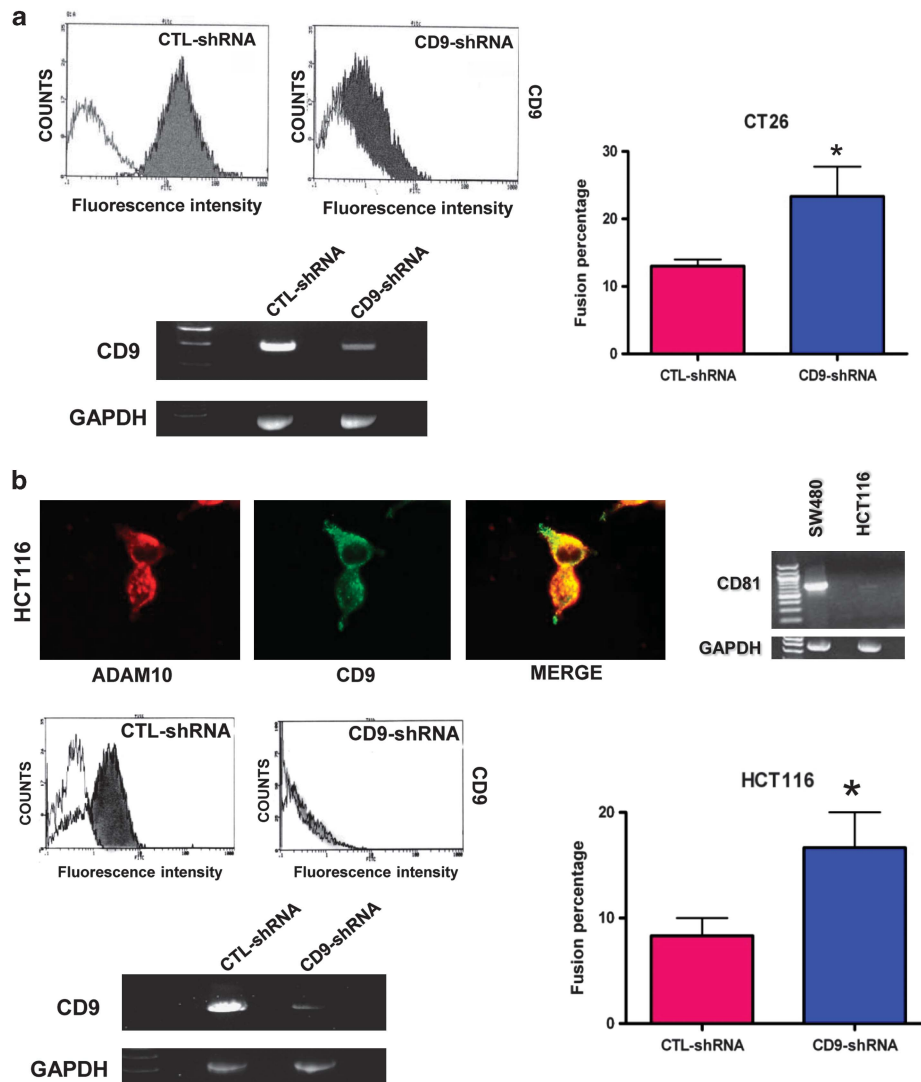


Figure 3. CD9 knockdown in CT26 and HCT116 cells results in augmented fusion ability. **(a)** Retrovirally transduced CT26 with a negative control shRNA (CTL-shRNA) and a shRNA targeted against the coding region of the mouse *CD9* gene (CD9-shRNA) were selected in puromycin-containing medium and, after 1–2 weeks, the decreased expression of CD9 protein and mRNA was assessed by flow cytometry and RT-PCR. The endogenous *GAPDH* mRNA level was measured as internal control, (left panels). Next, CD9-silenced CT26 were stably transfected with EGFP and mixed with CT26 stably transfected with RFP in the presence of geneticin. Fused cells were identified by dual color FACScan. Each bar represents the mean \pm s.d. * $P < 0.05$ (right panel). **(b)** Human colon carcinoma HCT116 cells, with endogenous expression levels of ADAM10 and CD9 but not expressing CD81 (upper panels) were retrovirally transduced with a negative control (CTL-shRNA) and with a shRNA against human CD9 (CD9-shRNA). Decreased expression levels of CD9 protein and mRNA were assessed by flow cytometry and RT-PCR. The endogenous *GAPDH* mRNA level was measured as internal control, (left panels). Next, CD9-silenced HCT116 were stably transfected with EGFP and mixed with HCT116 stably transfected with RFP in the presence of geneticin. Fused cells were identified by dual color FACScan. Each bar represents the mean \pm s.d. * $P < 0.05$ (right panel).

As shown in Supplementary Figure S3A, we noticed a significant colocalization of both proteins CD81 and $G\alpha 13$ to the juxtaposition of cell membrane. Next, we evaluated the cellular localization of ADAM10-RFP and CD81-GFP (Supplementary Figure S3B). We observed that ADAM10-RFP is localized in both intracellular vesicles and at cell–cell contact, and that this cellular distribution was paralleled by CD81-GFP. Similarly, colocalization of ADAM10-RFP with EGFP- $G\alpha 13$ was evident around the cell membrane confirming in living cells the findings observed analyzing the endogenous proteins (Supplementary Figure S3C).

Interaction of SW480 and CT26 with ADAM10 stimulates RhoA activity

As the interaction of $G\alpha 13$ with RhoA leads to an increase in cell cortical tension as well as in disruption of plasma

membrane–cortical actin,^{22,23} we investigated whether the interaction of SW480 and CT26 cells with ADAM10Cys-EGFP or ADAM10-EGFP activates Rho small GTPase. To this end, we performed a GTP-RhoA pull-down assay. First, we observed a colocalization of endogenous CD81 with RhoA to the plasma membrane in SW480 and CD9 with RhoA in CT26 cells (Figure 6a). Similarly, endogenous ADAM10 is colocalized with RhoA to the plasma membrane in SW480 and CT26 cells (data not shown). Second, SW480 and CT26 cells stimulated with ADAM10Cys-EGFP or ADAM10-EGFP resulted in increased levels of GTP-RhoA. Increased levels of GTP-RhoA were also obtained with the ectopic expression of $G\alpha 13$ in the same cell lines (Figure 6b). These data indicate that CD81/CD9/ADAM10 or CD9/ADAM10 complexes stimulates RhoA activity in interacting cells and disclose an involvement of $G\alpha 13$ in this process.

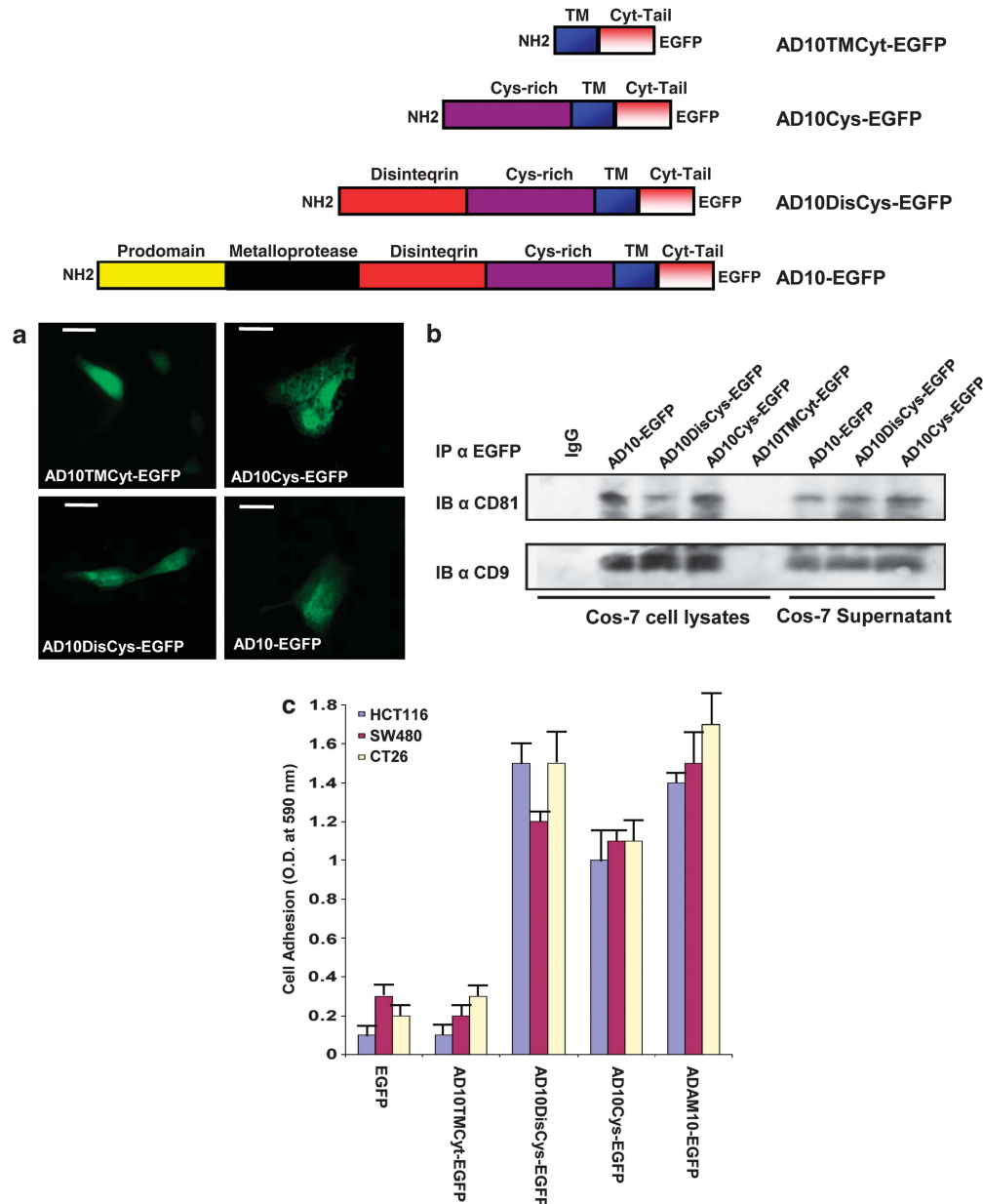


Figure 4. ADAM10 association with CD81 and CD9 requires cysteine-rich domain. **(a)** EGFP-tagged ADAM10 truncation mutants were expressed in COS-7 cells. **(b)** The association between ADAM10 and CD81 was analyzed by co-immunoprecipitation (IP) in both cell lysates and culture medium supernatants. CD81 (upper panel) was detected in immunoprecipitates of lysates from full-length ADAM10-, DisCys ADAM10- and CysADAM10-expressing cells but not in those from TMCyt ADAM10. The lower panel shows the presence of endogenous CD9 in the immunoprecipitates of full-length ADAM10, DisCys ADAM10 and CysADAM10. One representative experiment out of three is shown. **(c)** Colon carcinoma cells adhesion to ADAM10. HCT116, SW480 and CT26 were plated onto dishes coated with ADAM10-EGFP, ADAM10DisCys-EGFP, ADAM10Cys-EGFP or ADAM10TMCyt-EGFP as described in Materials and methods. Each bar represents the mean \pm s.d. of triplicate wells of three independent experiments.

ADAM10 causes $G\alpha_{13}$ -dependent myosin light-chain phosphorylation in colon carcinoma cells

The cell cortex is a network of cross-linked actin filaments whose tension levels are modified by external or internal cues. The cortical tension in cancer cells is mainly regulated by phosphorylation of the myosin light chain 2, also referred to as myosin regulatory light chain. Thus, we evaluated the levels of phospho-myosin light chain 2 (Ser19) in SW480 and CT26 cells after plating onto dishes coated with ADAM10Cys-EGFP or ADAM10-EGFP. We found that SW480 and CT26 plated on ADAM10-EGFP-coated dishes display increased levels of MLC2 phosphorylation, whereas cells lacking $G\alpha_{13}$ as a consequence of knockdown by siRNA

showed a remarkable reduction of phosphorylation of the myosin light chain 2 (Ser19) (Figures 6a and d). These data clearly demonstrate that the interaction of cells with ADAM10 causes phosphorylation of MLC2 and that the interaction of $G\alpha_{13}$ with RhoA positively influences this final event leading to an increase in myosin ATPase activity and cell contraction.²⁴

Reduced phosphorylation levels of ERM proteins following interaction of SW480 and CT26 with ADAM10

Cortical contractility is exceptionally high in tumor cells and the tension build up can induce disruption of the cell cortex at sites

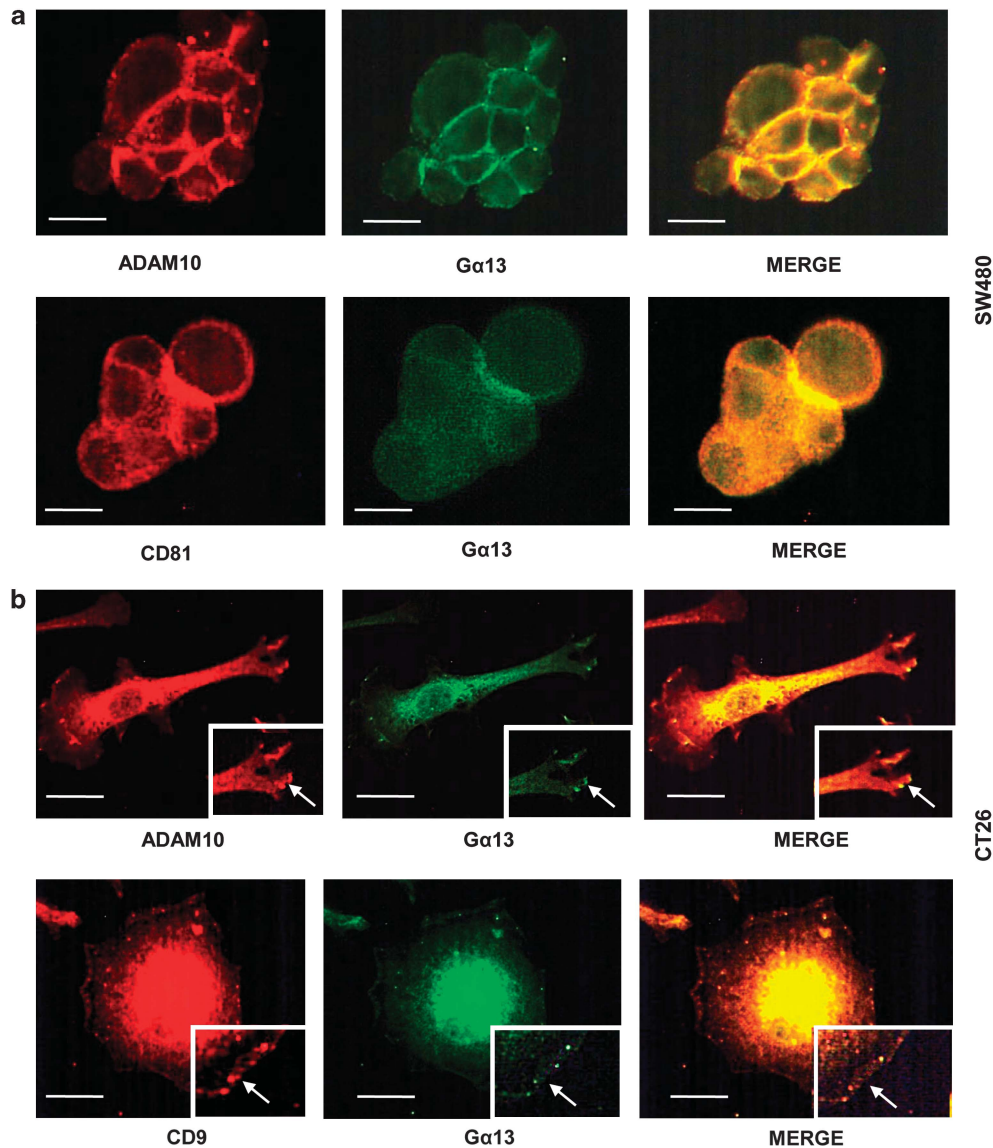


Figure 5. GTP-binding $\alpha 13$ protein associates to components of tetraspanin CD81/CD9 multi-protein complex. **(a)** Representative images showing endogenous ADAM10, CD81 and $G\alpha 13$ staining in SW480 cells. Staining shows a prominent colocalization of ADAM10 and CD81 with $G\alpha 13$. **(b)** Representative images showing endogenous ADAM10, CD9 and $G\alpha 13$ staining in CT26 cells. Staining shows a robust colocalization of ADAM10 and CD9 with $G\alpha 13$. Inset magnifies the colocalization of proteins to the plasma membrane. Scale bars, 20 μm .

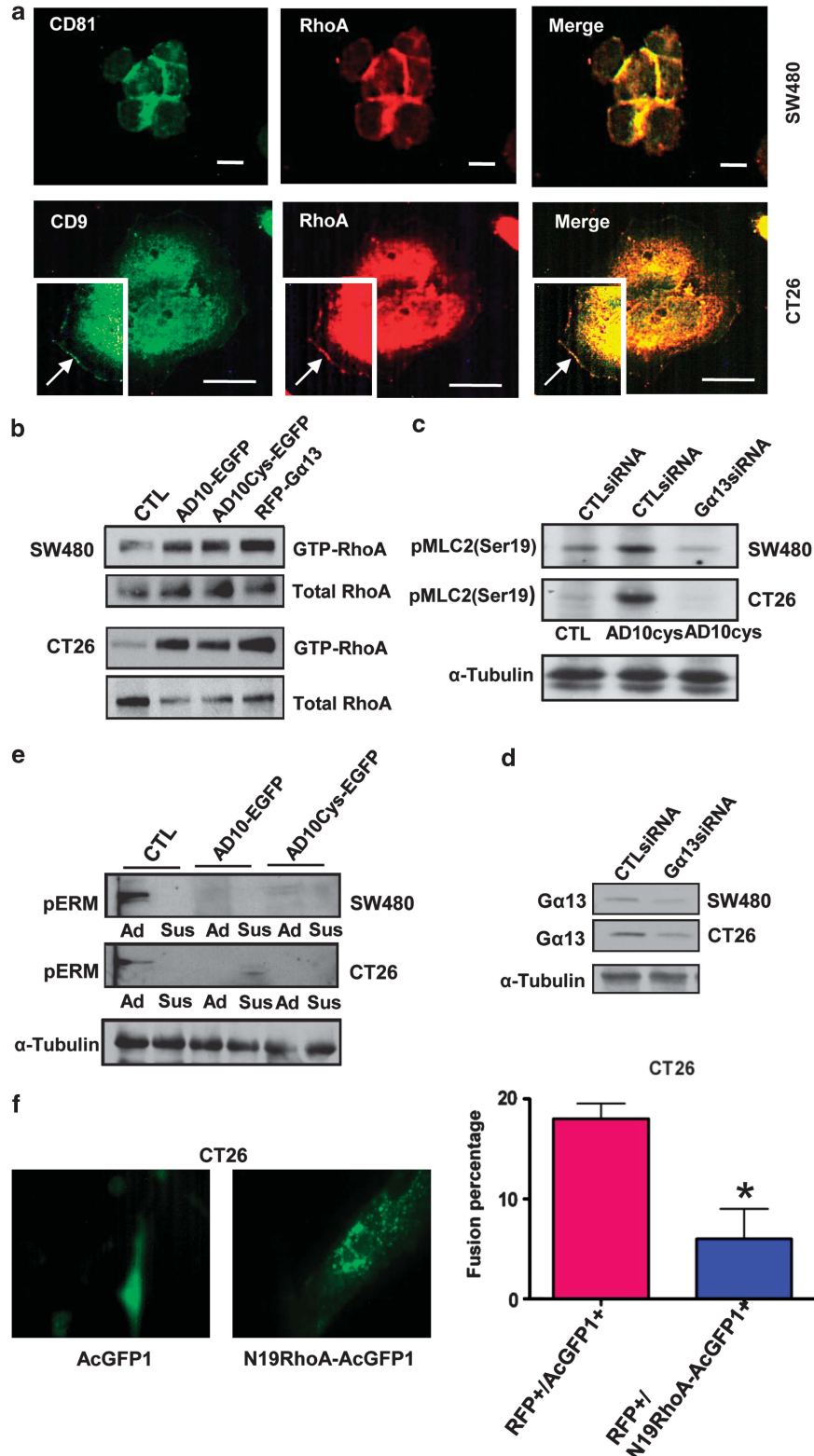
where plasma membrane and cortical actin interactions are locally reduced. In this regard, the ERM proteins (ezrin, radixin and moesin) function as linkers between the plasma membrane and the actin cytoskeleton, thus providing structural strength to the cell cortex.²⁵ Phosphorylation at a carboxy-terminal threonine residue (Thr567 of ezrin, Thr564 of radixin, Thr558 of moesin), which disrupts their amino- and carboxy-terminal association, has a key role in modulating the conformation and function of ERM proteins.²⁶ To this end, we evaluated the phosphorylation levels of ERM proteins using SW480 and CT26 cells plated onto ADAM10Cys-EGFP- or ADAM10-EGFP-coated dishes or maintained in suspension. As shown in Figure 6e, cells plated onto plastic revealed the presence of two phosphorylated proteins. In particular, the upper band corresponding to radixin/ezrin was strongly phosphorylated in both SW480 and CT26 cell lines. Conversely, when the cells were plated onto ADAM10Cys-EGFP and ADAM10-EGFP or maintained in suspension for 60 min phosphorylation of proteins was undetected. Taken together, these data suggest that the interactions of CD81/CD9/ADAM10 or

CD9/ADAM10 complexes in opposing fusogenic cancer cells increase cortical tension and initiate events of cortical actin membrane destabilization at the cell-cell contact that eventually induce cell fusion. Thus, to analyze a possible involvement of $G\alpha 13$ -Rho pathway in the aforementioned mechanism, we used a dominant-negative variant of Rho (N19RhoA), in which Ser19 is changed to Asn (N). The ectopic expression of N19RhoA has been demonstrated to inhibit endogenous Rho function and the $G\alpha 13$ -RhoA pathway by forming non-productive complexes with guanine nucleotide exchange factors (GEFs) for Rho.²⁷ The ectopic expression of N19RhoA significantly reduced the percentage of fused CT26 cells whereas the expression of control acGFP1 vector had no effect (Figure 6f).

Appearance of drug resistant to both 5-FU and Oxa as a consequence of cell fusion in metastatic colon carcinoma
We next sought to investigate the involvement of cell fusion in selecting chemoresistant cells to 5-FU and Oxa in metastatic colon

carcinoma. To this end, we transduced both CT26 cells, resistant to 5-FU, and CT26 cells resistant to Oxa with RFP and GFP retroviral vectors, respectively, or with ADAM10 cysteine domain-GFP (AD10CysGFP). Syngeneic mice were injected with a mixed cell population of RFP- and AD10CysGFP-CT26-positive cells or with a mixed population of RFP- and GFP-CT26-positive cells as control.

As expected, parental CT26 cells showed an aggressive behavior as demonstrated by the massive presence of metastatic nodules in the liver within 2 weeks after intrasplenic inoculation (Figure 7a). The cells isolated from metastatic nodules were treated with 5-FU, Oxa or with both drugs and cell survival then analyzed by dual color FACScan. As shown in Figure 7b, CT26-OxaR fused



spontaneously with CT26-5FUR *in vivo*. In addition, the ectopic expression of cysteine-rich domain ADAM10 increased the number of fused cells resistant to both 5-FU and Oxa in liver metastases from colon cancer (Figure 7c). We observed an average fusion percentage of 9.8% in RFP⁺/GFP⁺ mixed cell population and 18.4% in RFP⁺/AD10CysGFP⁺ (Figure 7d). Taken together, these data demonstrate the occurrence of cell fusion in metastatic colon carcinoma as well as the involvement of cell fusion in the appearance of tumor cell subpopulations resistant to both 5-FU and Oxa.

DISCUSSION

Colon cancer can usually be cured by surgical excision at any stage before metastases to distant sites (i.e., liver, lung) are established. Understanding the basic aspects of this process has obvious and important implications for clinical research. However, many questions still remain. For example, how many mutations are required for a particular metastatic cell population to acquire a widespread chemoresistance? Recent studies have established that the great majority of the mutations present in metastases are also present in the primary colon carcinoma. In addition, the process of *ex vivo* cell culture of tumors excised from patients does not introduce new mutations into colon tumor cell populations.^{28,29} It is reasonable that an alternative mechanism must be involved in this process and that, in this context, cell fusion contributes to widespread chemoresistance by combining genes responsible for resistance to various drugs. Here, we have shown that cell fusion is driven by ADAM10 in colon carcinoma and this induces chemoresistance to both 5-FU and Oxa. Fusion between tumor cells with distinct phenotypes can generate cells with new properties at a rate exceeding that achievable by random mutagenesis, thereby allowing a better adaptation to survive to the therapeutic treatments. Metastatic subpopulations might thus be more able to evolve under selective pressures than non-metastatic cells, by a process other than mutation.³⁰

Recent findings showing that chronic inflammation dramatically increases the frequency of cell fusion of hematopoietic cells with various cell lineages^{31,32} may account for the high fusogenicity of metastatic tumor cells, as inflammation is often associated with the tumor microenvironment and metastatic cells may trigger an inflammatory response once they colonize the liver. Recently, it has also been described that metastatic tumor cells are able to induce TNF- α production by Kupffer cells and these latter constitute the major source of TNF- α in tumor cell-inoculated livers.³³ In agreement with the aforementioned observations, our results show that metastatic cancer cells fuse spontaneously *in vitro* and *in vivo*. This is in line with another recent report by Lu and Kang showing that organotropisms of metastatic cells can be acquired through spontaneous fusion between cancer cells with bone and lung tropism that eventually generates populations of

cells capable of metastasizing to both organs.¹³ Finally, our study discloses a mechanism by which ADAM10 promotes fusion in colon cancer cells. Along this line, we propose that in a context of fusogenic cancer cells, ADAM10 may initiate a combination of events that lead to local disruption of interactions between plasma membrane and cortical actin and the consequent plasma membrane fusion. The role of ADAM10 in regulating plasma membrane-cortical actin at sites of cell-cell contact is particularly important in three-dimensional environments and *in vivo*. In addition, our study highlights that enhanced expression of ADAM10 in colon cancer cells has biological consequences that can be attributed to the presence of additional non-catalytic ADAM10 domains (i.e., cysteine-rich domain). This further implies that not all functions of ADAM10 in colon cancer cells will be abolished by effective protease inhibitors. Here we have also found that both G α 13 and Rho activity contribute to cell fusion through an increase in cell cortical tension as well as in disruption of plasma membrane-cortical actin interactions. Our study demonstrates not only the implication of ADAM10 in stimulating G α 13-mediated activation of RhoA and phosphorylation of myosin regulatory light chain, but it also shows a G α 13-dependent regulation of ERM proteins. It has been reported that G α 13 directly interacts with radixin, a member of ERM proteins, and that this interaction results in a conformational activation of radixin.³⁴ This phenomenon is possibly due to competition between components of the Rho signaling pathway (for example, p115 Rho GEF) and radixin for G α 13 binding, (see Figure 8). Finally, these findings emphasize the role that ADAM10 and the cytoskeleton play in promoting metastatic cancer cell fusion.

In conclusion, this study demonstrates a crucial role for cell fusion in colon carcinoma that makes cancer cells more resistant to conventional chemotherapeutic agents. The information derived from this study may have two relevant immediate consequences in the development of more efficient pharmacological strategies against metastatic colon cancer. First, the possibility of targeting hidden actions of multi-task metalloproteases such as ADAM10, and particularly its contribution to cancer cell fusion. Second, a better understanding of the biology of fused cancer cells will contribute to identify and employ specific inhibitors in the treatment of colon cancer.

MATERIALS AND METHODS

Cell lines and antibodies

SW480 and HCT116 human colon carcinoma cell lines, CT26 murine colon carcinoma cell line were purchased from ATCC (Rockville, MD, USA). Cos-7 cells were from ATCC.

Expression of ADAM10 truncation mutants

The plasmid pcDNA3-ADAM10 coding for wild-type bovine ADAM10 (GenBank: Z21961.1) was used as template to clone and insert ADAM10

Figure 6. CD81/CD9/ADAM10 complex stimulates RhoA activity, G α 13-dependent myosin light chain phosphorylation and reduces phosphorylation of ERM proteins. **(a)** Immunofluorescence staining showing the localization of CD81 with RhoA in SW480 and CD9 with RhoA in CT26 cells plated on cover slips coated with ADAM10Cys-EGFP. Inset magnifies the colocalization of proteins to the plasma membrane. Scale bars, 20 μ m. **(b)** SW480 and CT26 cells were plated on ADAM10-EGFP, ADAM10Cys-EGFP captured on plastic dishes through a coating of the wells with antibodies directed against the tagging protein EGFP. Proteins from lysates were immunoblotted with antibodies directed against RhoA. GTP-bound RhoA was measured by association with GST-Rhotekin rho-binding domain (GST-RBD) beads. RFP-G α 13 notation means ectopic expression of protein. CTL notation means coating of dishes with antibodies anti-EGFP. **(c)** G α 13 siRNA-transfected SW480 and CT26 cells were plated on ADAM10Cys-EGFP (AD10cys) captured on plastic dishes through a coating of the wells with antibodies directed against the tagging protein EGFP. Proteins from lysates were immunoblotted with antibodies to phospho-myosin light chain 2 (Ser19). CTL-siRNA notation means scrambled siRNA-transfected cells. **(d)** Immunoblot of SW480 and CT26 cell lysates showing reduced levels of G α 13 when this protein is knocked down. α -tubulin represents the loading control. **(e)** SW480 and CT26 cells were plated onto dishes coated with a supernatant of ADAM10-EGFP-transfected Cos-7 cells, with a supernatant of ADAM10Cys-EGFP transfectants or with a supernatant of Cos-7 cells maintained in suspension. Cells were then lysed and extracted proteins immunoblotted with antibodies to phospho-Ezrin (Thr567)/Radixin(Thr564)/Moesin(Thr558). **(f)** The column bar graph represents the percentage of CT26 fused cells measured in a mixed population of cells transduced with RFP⁺/AcGFP1⁺ and RFP⁺/N19RhoA-AcGFP1⁺. Each bar represents the mean \pm s.d. **P* < 0.01.

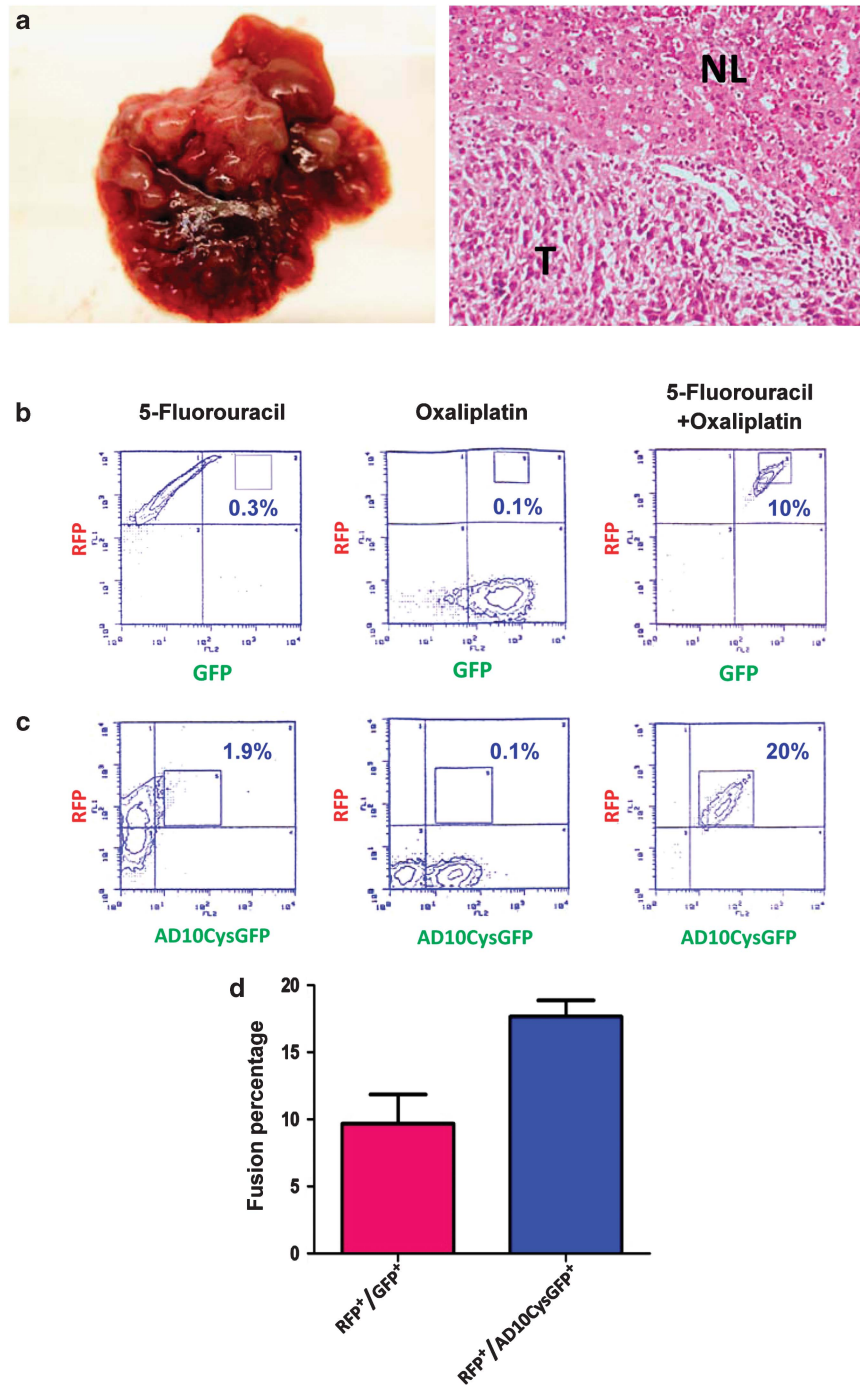


Figure 7. Cell fusion in selecting chemoresistant cells to 5-FU and Oxa in a syngeneic metastatic model of colon carcinoma. **(a)** A representative pattern of liver metastases following intrasplenic inoculation of wild-type CT26 in syngeneic mice is shown (left panel). Hematoxylin and eosin staining of a representative liver section showing a metastatic colon carcinoma lesion (right panel) NL, normal liver; T, tumor. **(b)** Syngeneic mice were injected with CT26 cells resistant to 5-FU labeled with RFP (left panel), CT26 cells resistant to Oxa labeled with GFP (middle panel) or with a mixed cell population of RFP and GFP CT26-positive cells (right panel). The cells isolated from the metastatic nodules were treated with 5-FU, Oxa or with both drugs and cell survival analyzed by dual color FACScan. RFP⁺, GFP⁺ and RFP⁺/GFP⁺ events were gated and shown as contour plot. **(c)** Syngeneic mice were injected with CT26 cells resistant to 5-FU labeled with RFP, CT26 cells resistant to Oxa labeled with ADAM10 cysteine-rich domain-GFP (AD10CysGFP) or with a mixed cell population of RFP and AD10CysGFP CT26-positive cells. The cells isolated from metastatic nodules were treated with 5-FU, Oxa or with both drugs and cell survival analyzed by dual color FACScan. RFP⁺, AD10CysGFP⁺ and RFP⁺/AD10CysGFP⁺ events were gated and shown as contour plot. **(d)** The column bar graph represents the percentage of fused cells measured as double-positive cells divided by total number of cells selected within the setting limits of flow cytometer.

into pEGFP-N1 (Clontech, Mountain View, CA, USA) or pTagRFP-N1 (Evrogen, Moscow, Russia) plasmids and for the construction of ADAM10 truncation mutants by PCR using *XhoI* and *KpnI* restriction enzymes.

Cell adhesion assay

Cell culture 24-well plate were coated with an anti-EGFP antibody by placing the antibody dilution (30 µg/ml) in the well plate.³⁵ The plate was

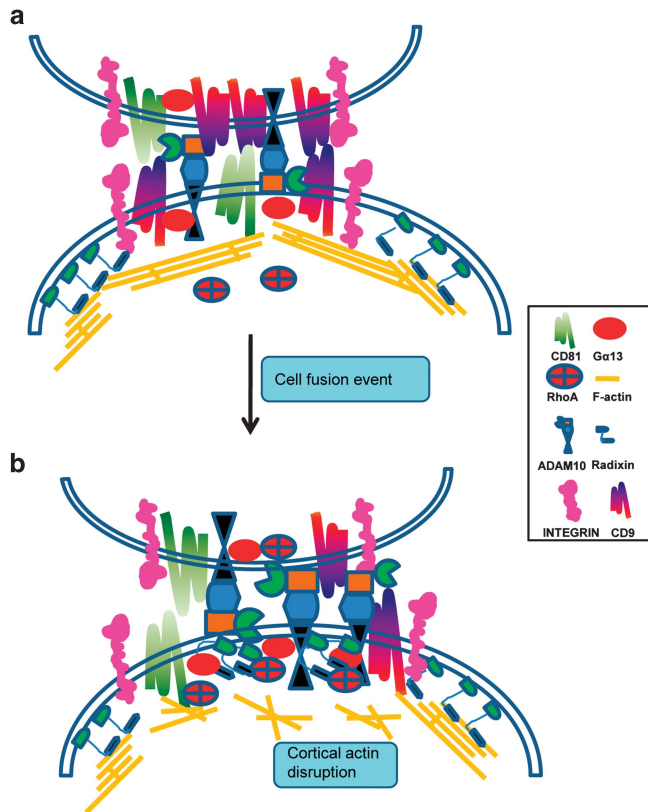


Figure 8. Model for CD81/CD9/ADAM10 regulation of metastatic colon cancer cell fusion. **(a)** Tetraspanin CD81/CD9 and ADAM10 contribute to bringing the opposing membranes into close proximity in fusing cancer cells and recruit intracellular proteins forming multi-protein complexes at the sites of fusion. **(b)** Enhanced expression of ADAM10 associated with low levels of CD81/CD9 causes Gα13-mediated activation of RhoA. RhoA activity elicits dephosphorylation of ERM protein radixin and disruption of plasma membrane-cortical actin interactions.

gently rocked overnight at 4 °C before the solution was aspirated. The protein binding sites of each well was blocked with sterile phosphate-buffered saline (PBS) containing 3% (w/v) BSA for 60 min at 37 °C. The blocking solution was aspirated and replaced with PBS as control or supernatant of Cos-7 transfected with ADAM10-EGFP, ADAM10DisCys-EGFP, ADAM10Cys-EGFP or ADAM10TMCyt-EGFP. The coating with supernatant was performed at 37 °C for 60 min. After a rinse with PBS, 500 μl of the cell suspension (5×10^4 /ml) was added to the wells for 60 min at 37 °C. The plate was rinsed twice in serum-free Dulbecco's modified Eagle medium and the cells fixed for 5 min in methanol, rinsed in PBS and stained with 0.1% crystal violet in 10% methanol (vol/vol). Absorbance was measured with an ELISA reader (Bio-Rad, Hercules, CA, USA) at 590 nm. A blank value corresponding to an empty well was automatically subtracted.

Flow cytometry and time-lapse confocal microscopy

For flow cytometry analysis, CT26 or HCT116 stable transfectants expressing EGFP or ADAM10-RFP were obtained by selection with geneticin. CT26-EGFP stable transfectants (10^6 cells) were mixed with CT26-ADAM10-RFP stable transfectants (10^6 cells) in the presence of geneticin. Fused cells were identified by dual color FACScan. For time-lapse microscopy experiments, we suspended an equal number of untransfected CT26 cells with ADAM10-RFP-transfected CT26 cells onto a layer of Matrigel plated on 60-mm glass-bottomed cell culture plates. Live imaging was performed at 37 °C using a Leica TCS SP2 confocal microscope with an aerated incubation chamber for long-term experiments with living cells. For immunofluorescence microscopy, cells were washed with PBS, fixed with 2.5% paraformaldehyde for 10 min, and then blocked 1 h with 3% goat normal serum in 0.05% Triton X-100. Cells were sequentially incubated with primary and Cy3- or Cy2-conjugated secondary antibodies.

Retroviral infections

We cloned by PCR the *EcoRI*- and *Sall*-flanked insert from plasmid pRetroQ ADAM10-GFP containing ADAM10 Cys-rich domain-GFP cDNA into retroviral vector pBabe-puro (Addgene, Cambridge, MA, USA). Furthermore, we cloned the *EcoRI* and *XhoI*-flanked fragment from vector pRetroQ-DsRed_{monomer} (Clontech), containing the full-length monomeric RFP cDNA, into retroviral vector pLXSN (Clontech).

Cell fusion in a syngeneic model of murine colon cancer metastasis

The cell lines CT26-OxaR and CT26-5FUR resistant, respectively, to chemotherapeutic drugs Oxa and 5-FU were obtained by selection in increasing concentrations of Oxa 10–25 μM and 5-FU 7.5–15 μM. CT26-OxaR and CT26-5FUR were infected with virus-containing supernatant and observed at least for two passages *in vitro* to verify that fluorescence intensity was stably expressed. CT26-OxaR expressing RFP, CT26-5FUR expressing GFP, CT26-5FUR expressing ADAM10 CysGFP or an equal mixture of these cells were injected into mice. Six-week-old male BALB/c mice were purchased from Charles River Laboratories (Lecco, Italy) and liver metastases were generated by intrasplenic injection of 1×10^5 cells in PBS (50 μl). After 2 weeks, the livers were removed and the extracted metastases plated on dishes were cultured under sterile conditions. Outgrown cells were treated for a week with both 25 μM of Oxa and 15 μM of 5-FU to select for resistant cells and the survival cells were analyzed by dual color flow cytometry.

Statistical analysis

All data are expressed as means ± s.d. Statistical analysis was performed by Student's *t*-test (analysis with GraphPad Prism).

CONFLICT OF INTEREST

The authors declare no conflict of interest.

ACKNOWLEDGEMENTS

We thank Peter Altevogt and Joaquin Teixidò for important reagents used in this study. This work was supported by grant from Ente Cassa di Risparmio di Firenze.

REFERENCES

- Borst P, Schinkel AH, Smit JJ, Wagenaar E, Van Deemter L, Smith *et al*. Classical and novel forms of multidrug resistance and the physiological functions of P-glycoprotein in mammals. *Pharmacol Ther* 1993; **60**: 289–299.
- Cole SP, Sparks KE, Fraser K, Loe DW, Grant CE, Wilson GM *et al*. Pharmacological characterization of multidrug resistant MRP-transfected human tumor cells. *Cancer Res* 1994; **54**: 5902–5910.
- Samimi G, Manorek G, Castel R, Breaux JK, Cheng TC, Berry CC *et al*. cDNA microarray-based identification of genes and pathways associated with oxaliplatin resistance. *Cancer Chemother Pharmacol* 2005; **55**: 1–11.
- Meyerhardt JA, Mayer RJ. Systemic therapy for colorectal cancer. *N Engl J Med* 2005; **352**: 476–487.
- André T, Boni C, Mounedji-Boudiaf L, Navarro M, Taberero J, Hickish T *et al*. Oxaliplatin, fluorouracil, and leucovorin as adjuvant treatment for colon cancer. *N Engl J Med* 2004; **350**: 2343–2351.
- Alberts SR, Horvath WL, Sternfeld WC, Goldberg RM, Mahoney MR, Dakhil SR *et al*. Oxaliplatin, fluorouracil, and leucovorin for patients with unresectable liver-only metastases from colorectal cancer: a North Central Cancer Treatment Group Phase II Study. *J Clin Oncol* 2005; **23**: 9243–9249.
- Duelli D, Lazebnik Y. Cell fusion: a hidden enemy? *Cancer Cell* 2003; **3**: 445–448.
- Duelli D, Lazebnik Y. Cell-to-cell fusion as a link between viruses and cancer. *Nat Rev Cancer* 2007; **7**: 968–976.
- Lu X, Kang Y. Cell fusion as a hidden force in tumor progression. *Cancer Res* 2009; **69**: 8536–8539.
- Fortuna MB, Dewey MJ, Furmanski P. Cell fusion in tumor development and progression: occurrence of cell fusion in primary methylcholantrene-induced tumorigenesis. *Int J Cancer* 1989; **44**: 731–737.
- Fortuna MB, Dewey MJ, Furmanski P. Enhanced lung colonization and tumorigenicity of fused cells isolated from primary MCA tumors. *Cancer Lett* 1990; **55**: 109–114.
- Wakeling WF, Greetha J, Bennett DC. Efficient spontaneous fusion between some co-cultured cells, especially murine melanoma cells. *Cell Biol Int* 1994; **18**: 207–210.

- 13 Lu X, Kang Y. Efficient acquisition of dual metastasis organotropism to bone and lung through stable spontaneous fusion between MDA-MB-231 variants. *Proc Natl Acad Sci USA* 2009; **106**: 9385–9390.
- 14 Chen HE, Olson NE. Unveiling the mechanisms of cell-cell fusion. *Science* 2005; **308**: 369–373.
- 15 Tachibana I, Hemler ME. Role of transmembrane 4 superfamily (TM4SF) proteins CD9 and CD81 in muscle cell fusion and myotube maintenance. *J Cell Biol* 1999; **146**: 893–904.
- 16 Takeda Y, Tachibana I, Miyado K, Kobayashi M, Miyazaki T, Funakoshi T *et al*. Tetraspanins CD9 and CD81 function to prevent the fusion of mononuclear phagocytes. *J Cell Biol* 2003; **161**: 945–956.
- 17 Parthasarathy V, Martin F, Higginbottom A, Murray H, Moseley GW, Read RC *et al*. Distinct roles for tetraspanins CD9, CD63 and CD81 in the formation of multinucleated giant cells. *Immunology* 2008; **127**: 237–248.
- 18 Wolfsberg TG, Primakoff P, Myles DG, White JM. ADAM a novel family of membrane proteins containing A Disintegrin And Metalloprotease domain: multi-potential functions in cell-cell and cell-matrix interactions. *J Cell Biol* 1995; **131**: 275–278.
- 19 White MJ. ADAMs: modulators of cell–cell and cell–matrix interactions. *Curr Opin Cell Biol* 2003; **15**: 598–606.
- 20 Link AJ, Eng J, Schieltz DM, Carmack E, Mize GJ, Morris DR *et al*. Direct analysis of protein complexes using mass spectrometry. *Nat Biotechnol* 1999; **17**: 676–682.
- 21 Mazzocca A, Liotta F, Carloni V. Tetraspanin CD81-regulated cell motility plays a critical role in intrahepatic metastasis of hepatocellular carcinoma. *Gastroenterology* 2008; **135**: 244–256.
- 22 Klages B, Brandt U, Simon MI, Schultz G, Offermanns S. Activation of G α 12/G α 13 results in shape change and Rho/Rho-Kinase-mediated myosin light chain phosphorylation in mouse platelets. *J Cell Biol* 1999; **144**: 745–754.
- 23 Kelly P, Moeller BJ, Juneja J, Booden MA, Der CJ, Daaka Y *et al*. The G12 family of heterotrimeric G proteins promotes breast cancer invasion and metastasis. *Proc Natl Acad Sci USA* 2006; **103**: 8173–8178.
- 24 Paluch E, Sykes C, Prost J, Bornens M. Dynamic modes of the cortical actomyosin gel during cell locomotion and division. *Trends Cell Biol* 2006; **16**: 5–10.
- 25 Fehon RG, McClatchey AI, Bretscher A. Organizing the cell cortex: the role of ERM proteins. *Nat Rev Mol Cell Biol* 2010; **11**: 276–287.
- 26 Matsui T, Maeda M, Doi Y. Rho-kinase phosphorylates COOH-terminal threonines of Ezrin/Radixin/Moesin (ERM) proteins and regulates their head-to-tail association. *J Cell Biol* 1998; **140**: 647–657.
- 27 Hart MJ, Jiang X, Kozasa T, Roscoe W, Singer WD, Gilman AG *et al*. Direct stimulation of the guanine nucleotide exchange activity of p115 RhoGEF by G α 13. *Science* 1998; **280**: 2112–2114.
- 28 Jones S, Chen WD, Parmigiani G, Diehl F, Beerwinkel N, Antal T *et al*. Comparative lesion sequencing provides insights into tumor evolution. *Proc Natl Acad Sci USA* 2008; **105**: 4283–4288.
- 29 Wood LD, Parsons DW, Jones S, Lin J, Sjöblom T, Leary RJ *et al*. The genomic landscapes of human breast and colorectal cancers. *Science* 2007; **318**: 1108–1113.
- 30 Waghorne C, Thomas M, Lagarde A, Kerbel RS, Breitman ML. Genetic evidence for progressive selection and overgrowth of primary tumors by metastatic cell subpopulations. *Cancer Res* 1988; **48**: 6109–6114.
- 31 Johansson CB, Youssef S, Kolekar K, Holbrook C, Doyonnas R, Corbel SY *et al*. Extensive fusion of haematopoietic cells with Purkinje neurons in response to chronic inflammation. *Nat Cell Biol* 2008; **10**: 575–583.
- 32 Pawelek JM, Chakraborty AK. Fusion of tumor cells with bone marrow-derived cells: a unifying explanation for metastasis. *Nat Rev Cancer* 2008; **8**: 377–386.
- 33 Khatib AM, Auguste P, Fallavollita L, Wang N, Samani A, Kontogianna M *et al*. Characterization of the host proinflammatory response to tumor cells during the initial stages of liver metastasis. *Am J Pathol* 2005; **167**: 749–759.
- 34 Vaiskunaitė R, Adarichev V, Furthmayr H, Kozasa T, Gudkov A, Voynov-Yasenetskaya TA. Conformational activation of radixin by G13 protein α subunit. *J Biol Chem* 2000; **275**: 26206–26212.
- 35 Carloni V, Mazzocca A, Ravichandran KS. Tetraspanin CD81 is linked to ERK/MAPKinase signalling by Shc in liver tumor cells. *Oncogene* 2004; **23**: 1566–1574.

Supplementary Information accompanies the paper on the Oncogene website (<http://www.nature.com/onc>)